Crystal structure of a nuclear actin ternary complex

Tingting Cao[a,b], Lingfei Sun[a,b], Yuxiang Jiang[b], Shanjin Huang[b], Jiawei Wang[b,c], and Zhucheng Chen[a,b,1]

[a]Ministry of Education Key Laboratory of Protein Science, Tsinghua University, Beijing 100084, P.R. China; [b]School of Life Science, Tsinghua University, Beijing 100084, P.R. China; and [c]State Key Laboratory of Bio-membrane and Membrane Biotechnology, Tsinghua University, Beijing 100086, P.R. China

Edited by Carl Wu, Howard Hughes Medical Institute, Ashburn, VA, and approved June 21, 2016 (received for review February 25, 2016)

Actin polymerizes and forms filamentous structures (F-actin) in the cytoplasm of eukaryotic cells. It also exists in the nucleus and regulates various nucleic acid transactions, particularly through its incorporation into multiple chromatin-remodeling complexes. However, the specific structure of actin and the mechanisms that regulate its polymeric nature inside the nucleus remain unknown. Here, we report the crystal structure of nuclear actin (N-actin) complexed with actin-related protein 4 (Arp4) and the helicase-SANT–associated (HSA) domain of the chromatin remodeler Swr1. The inner face and barbed end of N-actin are sequestered by interactions with Arp4 and the HSA domain, respectively, which prevents N-actin from polymerization and binding to many actin regulators. The two major domains of N-actin are more twisted than those of globular actin (G-actin), and its nucleotide-binding pocket is occluded, freeing N-actin from binding to and regulation by ATP. These findings revealed the salient structural features of N-actin that distinguish it from its cytoplasmic counterpart and provide a rational basis for its functions and regulation inside the nucleus.

nuclear actin | Arp4 | chromatin remodeling | crystal structure

Actin self-assembles into a two-stranded filamentous structure (F-actin) in the cytoplasm, where it acts as a key component of the eukaryotic cytoskeleton. The polymerization of actin is regulated by the bound nucleotide and several actin-binding proteins (ABPs) (1). The binding of ATP promotes actin polymerization, whereas ADP-bound actin is susceptible to depolymerization. Numerous ABPs, including cofilin, profilin, and thymosin-β4, have been identified, and they regulate the dynamics of actin in the cytoplasm. The actin-related proteins (ARPs) are homologs of actin. Two of these, Arp2 and Arp3, form a tight complex (the Arp2/3 complex) and bind to the side of a mother filament to promote the formation of a branched F-actin structure (2).

Actin, several ARPs, and many ABPs are also found in the nucleus. The presence of actin in the nucleus was once considered controversial (3, 4). The most convincing evidence for the presence of N-actin in the nucleus comes from studies of chromatin regulatory complexes (5–8). Actin and Arp4 form a conjugated pair and are assembled into several chromatin-remodeling complexes, including the Swr1, Ino80, and BAF complexes, and the acetyltransferase NuA4 complex (9, 10). In addition to N-actin and Arp4, the Swr1 complex also contains Arp6, and the Ino80 complex contains Arp5 and Arp8. These chromatin-remodeling complexes are ATP-driven molecular machines that slide, remove, and reconstruct nucleosomes, thus regulating gene transcription, DNA repair, homologous recombination, and many other nucleic acid transactions (9). It is known that the Swr1 complex is responsible for reconstruction of the nucleosome through replacement of canonical H2A-H2B dimers with H2A.Z-H2B dimers, whereas the Ino80 complex performs diverse functions, including transcription activation and DNA repair (9). Deregulation of the chromatin-remodeling processes is associated with various human diseases, particularly cancers (11–13).

Although N-actin and Arp4 are widely conserved from yeast to humans, their specific structures and functions within the chromatin regulatory complexes remain largely unknown. N-actin and Arp4 are incorporated into different chromatin regulatory complexes through a common motif, the HSA domain (10). In yeast, the HSA domains of Snf2 and Sth1 bind to the Arp7/Arp9 pair, whereas those of Swr1, Ino80, and Eaf1 (a subunit of the NuA4 complex) specifically recognize the N-actin/Arp4 pair. Arp4 directly interacts with G-actin and inhibits its polymerization in solution (14). In yeast, Arp4 is suggested to interact with histone and target the NuA4 complex to the site of DNA damage (15, 16). BAF53/Actl6 (an Arp4 homolog in mammalian cells) regulates the recruitment of the BAF complex to the promoters of specific genes, controlling neural development, epidermal differentiation, and hematopoietic stem cell function (17–20).

Less is known about N-actin. The current understanding of N-actin is mostly related to the prior acknowledge of its well-studied counterpart in the cytoplasm (3, 21–23). Early studies suggested that N-actin within the BAF complex interacts with actin filaments, cofilin, and profilin (5, 24). By contrast, a recent study showed that N-actin within the Ino80 complex is in a monomeric state and does not bind profilin (25). Instead, N-actin might play a role in chromatin substrate handling. How N-actin is regulated by various nuclear ABPs is unclear.

In this study, we determined the structure of N-actin in complex with Arp4 and the HSA domain of Swr1 at a resolution of 2.8 Å. The structure illustrates the salient features of N-actin within the chromatin-remodeling complex, which distinguish it from cytoplasmic actin and provide the structural foundation for understanding its functions and regulation inside the nucleus.

Results and Discussion

Overall Structure of the Actin–Arp4–HSA^{swr1} Complex. We report the crystal structure of actin of the budding yeast *Saccharomyces cerevisiae* in complex with Arp4 and the HSA domain of the chromatin remodeler Swr1. Swr1 has an N-terminal HSA domain, which recognizes N-actin and Arp4, and a C-terminal ATPase core domain, which performs the key enzymatic reaction. The actin–Arp4–HSA^{Swr1} complex was reconstituted in vitro with actin and Arp4 expressed

Significance

Actin is a prominent component of the cytoskeleton in the cytoplasm of eukaryotic cells. Its presence in the nucleus was once considered controversial. However, it is now widely accepted that nuclear actin (N-actin) is a constitutive subunit of several chromatin-remodeling complexes. Yet, the specific structure of N-actin and how its polymerization is regulated remain unresolved. Our study presents the first crystal structure of the N-actin complex to our knowledge and illustrates the salient features that distinguish N-actin from its cytoplasmic counterpart. These features prevent the self-polymerization of N-actin and its regulation by many known actin-binding proteins. Our findings provide a rational basis for the functions of N-actin, laying the groundwork for future studies in this field.

Author contributions: Z.C. designed research; T.C., L.S., and Y.J. performed research; S.H., J.W., and Z.C. analyzed data; and Z.C. wrote the paper.

The authors declare no conflict of interest.

This article is a PNAS Direct Submission.

Data deposition: The atomic coordinates have been deposited in the Protein Data Bank, www.pdb.org (PDB ID code 5I9E).

[1]To whom correspondence should be addressed. Email: zhucheng_chen@tsinghua.edu.cn.

This article contains supporting information online at www.pnas.org/lookup/suppl/doi:10.1073/pnas.1602818113/-/DCSupplemental.

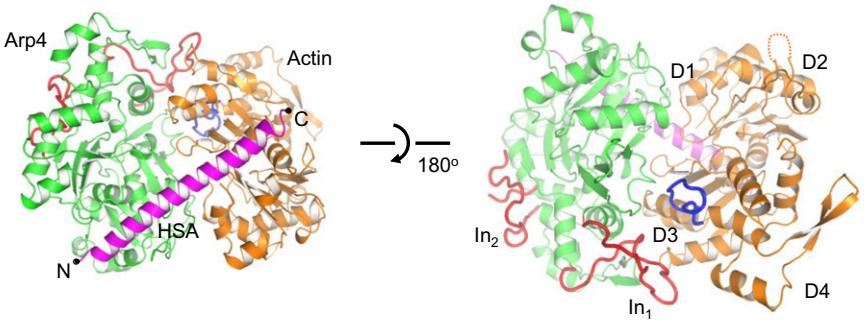

Fig. 1. Two different views of the overall structure of the actin–Arp4–HSA complex. Actin, orange; Arp4, green; HSA domain, magenta; the "hydrophobic plug" of actin, blue; the two insertions (In1 and In2) of Arp4, red. The N and C termini of the HSA domain are labeled with black dots. The four subdomains of actin are labeled D1, D2, D3, and D4.

individually in insect cells and the HSA domain of Swr1 expressed in *Escherichia coli* (Fig. S1). The final model was refined to 2.8 Å, with R_{work}/R_{feee} = 0.23/0.28 (Table 1).

The HSA domain functions as the key organizer in the assembly of the ternary complex. It forms a long helix, with its N and C termini binding to Arp4 and N-actin, respectively (Fig. 1). As suggested (26), the barbed end of N-actin interacts with the amphipathic HSA domain through its hydrophobic cleft. The DNase-I–binding loop in N-actin subdomain D2, which is suggested to be involved in chromatin binding (25), is disordered. The inner face of N-actin, including the "hydrophobic plug," makes multiple contacts with Arp4 (Fig. 1 and Fig. S2). The barbed end of actin is responsible for its longitudinal interactions within the actin filament, whereas the inner face of actin is responsible for its lateral interactions and is buried inside two-stranded F-actin (27–29). These key elements for F-actin assembly are sequestered by the interactions with Arp4 and the HSA domain, which provides the structural basis for preventing N-actin from polymerization. This structure is also consistent with an earlier study, which showed that Arp4 reduces the polymerization rate of G-actin and cannot bind to F-actin (14).

Interactions Between the HSA Domain and actin/Arp4. The structures of the yeast-specific ARPs, Arp7 and Arp9, when complexed with the HSA domain of the chromatin remodeler Snf2, have been reported (26). To compare these two HSA domain-containing complexes, we aligned the structures of Arp4 and Arp7 (Fig. 2*A*). This structural superposition leads to more accurate sequence alignments of the HSA domains (Fig. 2*B*), which mostly agree with the earlier result, except in the alignment of Snf2 and Ino80 (10). Consistent with a previous suggestion (26), the actin/Apr4 pair is organized in the same way as the Arp7/Arp9 pair, with Arp4 and actin located at the positions of Arp7 and Arp9, respectively (Fig. 2*A*). The sequence conservation of actin and the ARPs and the overall structure of the complex suggest that the actin/Arp4 and Arp7/9 modules have evolved from a common ancestor and have similar functions in the cell. Consistent with this notion, both the Arp7/9 and actin/Arp4 modules were shown to modulate chromatin remodeling activities in vivo and in vitro (10, 25, 30).

The HSA domain of Snf2 binds to Arp7 and Arp9, whereas the HSA domain of Swr1 binds to Arp4 and actin (10). Our structure reveals the specific recognition between different HSA helices and the N-actin/ARP pairs. The HSA^{Snf2} helix is longer than the HSA^{Swr1} helix, with the N-terminal end binding to the next molecule in the crystal lattice (26). In the structure of the N-actin complex, both the N and C termini of the HSA^{Swr1} helix are free of crystal packing interactions (Fig. S3). The N terminus of the HSA domain of Swr1, which involves three bulky residues (Leu355, Met362, and Phe366), binds the hydrophobic cleft and the N-terminal loop of Arp4, covering a large surface area of ∼1,200 $Å^2$ (Fig. 2*C*). By contrast, the HSA domain of Snf2 lacks two of the important hydrophobic residues (Met362 and Phe366) at the corresponding positions, and forms less-extensive contacts with Arp7, covering a smaller surface area of ∼600 $Å^2$. The C terminus of the HSA domain of Swr1, which involves three hydrophobic residues (Ala377, Val380, and Ile384), interacts with the hydrophobic cleft of N-actin (Fig. 2*D*). The structural superposition indicated that the longer C terminus of the HSA^{Snf2} helix mediates additional interactions with Arp9 that are not found at the HSA^{Swr1}–actin interface (Fig. 2*D*). In particular, Leu640 of HSA^{Snf2} makes hydrophobic contacts with Phe30 and Phe416 of Arp9. These results suggest that the N-actin/Arp4 and Arp7/Arp9 pairs recognize the unique compositions of the target HSA helices.

The HSA domains of Ino80 and Eaf1 also recognize the actin/Arp4 pair in yeast. Sequence alignments showed that residues with similar hydrophobic properties are found at most of the equivalent positions of the HSA domains of Eaf1 and Ino80 (Fig. 2*B*). These results suggest that the actin/Arp4/HSA module in the NuA4 and Ino80 complexes assembles in a way similar to the structure reported here.

Table 1. Data collection and refinement statistics

Data collection	
Space group	$P2_12_12$
Cell dimensions	
a, *b*, *c*, Å	110.260, 202.220, 87.010
α,β,γ, °	90.00, 90.00, 90.00
Resolution, Å	50–2.8 (2.87–2.8)*
R_{sym} or R_{merge}	0.115 (0.972)
$I/\sigma I$	15.4 (1.15)
Completeness, %	99.7 (99.2)
Redundancy	9.4 (3.9)
CC1/2	0.585
Refinement	
Resolution, Å	48.4–2.80
No. reflections	48,531
R_{work}/R_{free}	0.2317/0.2844
No. of atoms	
Protein	12,600
Ligand/ion	66
Water	0
B factors	
Protein	108
Ligand/ion	92
Water	/
rms deviations	
Bond lengths, Å	0.007
Bond angles, °	0.708

*Values in parentheses are for the highest-resolution shell.

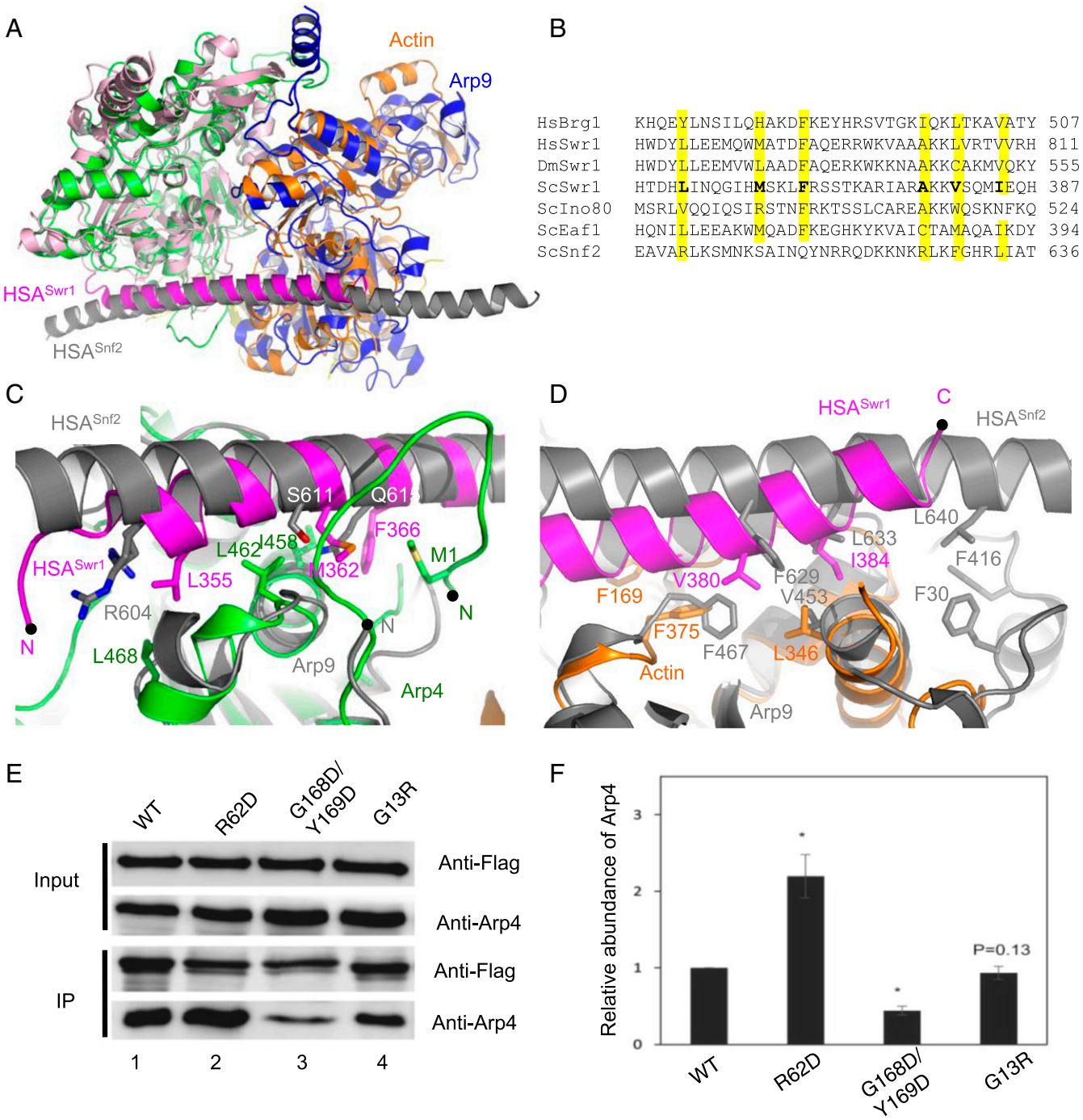

Fig. 2. Interactions between the HSA domain and actin/Arp4. (*A*) Superposition of the actin/Arp4 module with the Arp7/9 module. Arp7, pink; Arp9, blue; HSA domain of Snf2, gray. Arp4 and Arp7 were structurally aligned. (*B*) Multiple sequence alignments of the HSA domain. The residues involved in binding to Arp4 and actin are shown in bold (ScSwr1). The hydrophobic residues implicated in binding to N-actin and ARPs are highlighted in yellow. Dm, *Drosophila melanogaster*; Hs: *Homo sapiens*; Sc, *S. cerevisiae*. (*C*) Comparison of the HSA^{Swr1}–Arp4 interaction with the HSA^{Snf2}–Arp7 interaction. The structures of Arp4 and Arp7 are aligned. Three key hydrophobic residues of HSA^{Swr1} (L355, M362, and F366) are labeled, corresponding to R604, S611, and Q615 of HSA^{Snf2}, respectively. (*D*) Comparison of the interactions around the C termini of the HSA domains. The structures of N-actin and Arp9 are aligned. The C terminus of HSA^{Swr1} binds to the barbed end of N-actin and contacts multiple hydrophobic residues, including F169 (corresponding to Y169 in human β-actin), F375, and L346. Two key residues of HSA^{Swr1} (V380 and I384) are labeled. Similar hydrophobic interactions were also observed at the HSA^{Snf2}–Arp9 interface. (*E*) The coimmunoprecipitation of endogenous Arp4 with Flag-tagged actin in HEK293 cells. (*F*) Quantification of the normalized amounts of Arp4 coimmunoprecipitated with WT actin and three mutant actins. Error bars show the SEM of at least five independent experiments. $*P < 0.01$.

In human cells, N-actin and Arp4 bind to the HSA domains of the Swr1 homolog P400 and the Snf2 homolog Brg1 (10). Our structure suggests that they interact in a similar way. To test this model, we transfected human embryonic kidney (HEK) 293 cells with plasmids encoding Flag-tagged wild-type (WT) and mutant human β-actin, immunoprecipitated the Flag-tagged actin from the nuclear extract, and probed the coimmunoprecipitate for endogenous Arp4. As expected, we coimmunoprecipitated

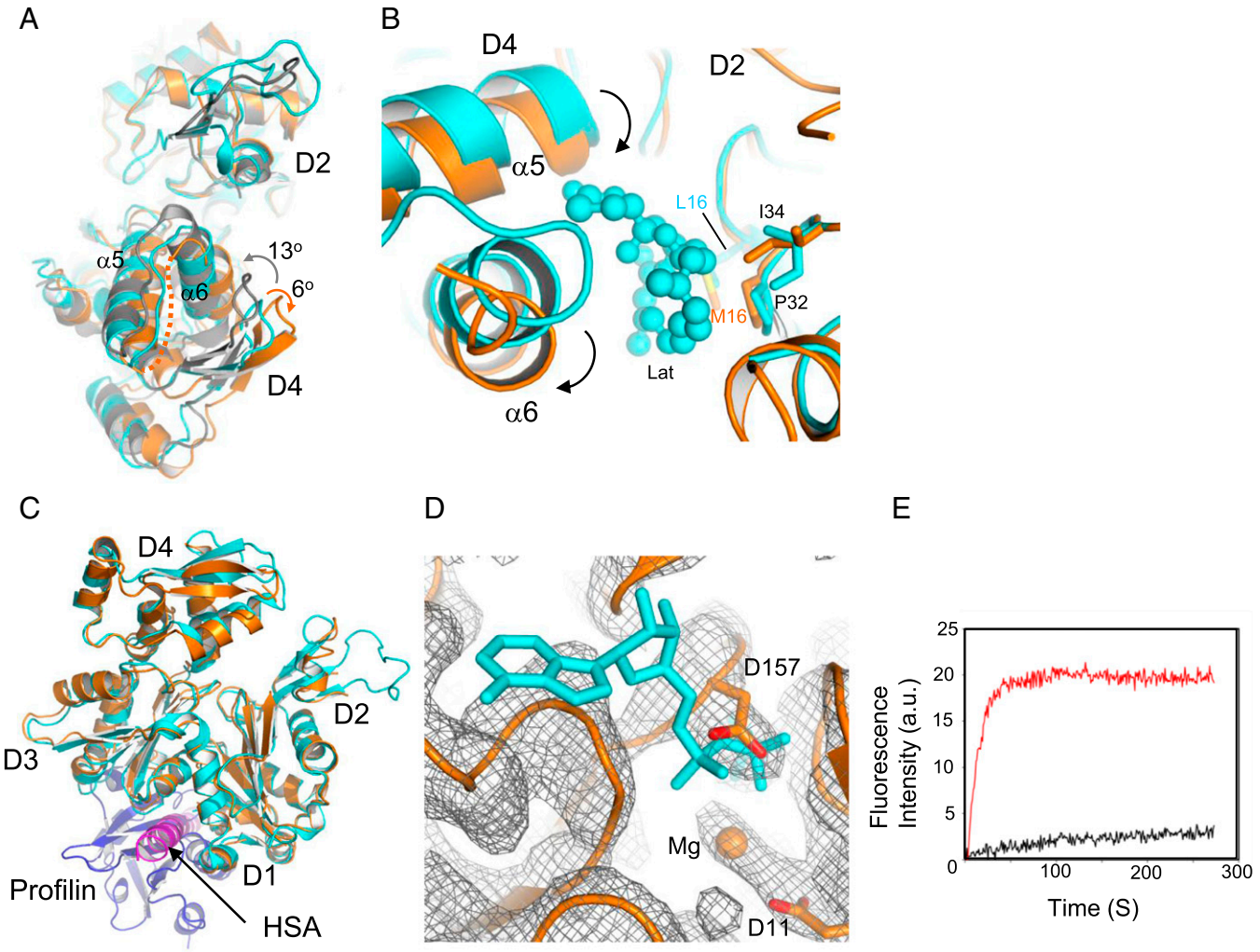

Fig. 3. Structural features of N-actin complexed with Arp4. (*A*) Superposition of N-actin (orange), G-actin [cyan; Protein Data Bank (PDB) ID code 1YAG], and an actin protomer in F-actin (gray, PDB ID code 3MFP). The structural alignments were constructed on the major domain D1–D2. Upon polymerization, the two major domains of G-actin show a counterclockwise rotation of ∼13° and become flat in F-actin, whereas it is additionally twisted by a clockwise rotation of ∼6° in the N-actin complex. (*B*) Conformational changes in the major-domain cleft of N-actin around the latrunculin-binding pocket. N-actin was structurally aligned with G-actin (PDB ID code 1ESV). Latrunculin (Lat), in a ball-and-stick model, is surrounded by hydrophobic contacts from L16, P32, and I34 in D2 subdomain of G-actin. The arrows indicated the movement of α5 and α6. (*C*) Superposition of the structures of N-actin and G-actin bound to profilin (blue; PDB ID code 2BTF). The HSA helix bound to the hydrophobic cleft of N-actin clashes with profilin. (*D*) Superposition of the structure of N-actin with the electron density map (contour level σ = 1) of the nucleotide-binding pocket. The ADP bound by G-actin (PDB ID code 1YAG) is indicated with a stick model. No electron density at the position of ADP was found in the crystal structure of the N-actin complex. (*E*) Time-course of the nucleotide exchange by G-actin (red curve) and the N-actin complex (black curve). Conditions: 3 μM G-actin or N-actin complex was mixed with 50 μM ε-ATP in buffer (2 mM Tris·HCl, pH 7.5 and 50 mM KCl).

endogenous Arp4 with WT actin, but at significantly lower levels when actin was mutated in the hydrophobic cleft (G168D/F169D) (Fig. 2 *E* and *F*) (29). By contrast, mutation R62D at the pointed end of actin, which prevents its polymerization but does not perturb its interaction with the HSA domain, enhanced the coimmunoprecipitation of Arp4. This enhancement is probably attributable to the nuclear enrichment of the mutant, as reported (31) (Fig. S4).

Structural Features of N-Actin. The two major domains of cytoplasmic G-actin (D1/D2 and D3/D4) are twisted, which become flat upon actin polymerization (27, 29). Interactions with Arp4 and the HSA domain twist the two major domains of N-actin by a further ∼6°, with the N terminus of the α6 helix (Thr202–Cys217) and the preceding loop becoming disordered (Fig. 3*A*). Consequently, the pointed end of N-actin is reshaped. The more-twisted major domains of N-actin inhibit the binding of another actin molecule to the pointed end, which provides an additional mechanism preventing actin from polymerization.

Several pointed end-binding proteins, including tropomodulin and thymosin-β4, bind to actin across the major-domain cleft and interact with α6 (32, 33). The conformational changes in N-actin hinder these interactions (Fig. S5). This cleft also binds several toxins, including latrunculin and phalloidin, which modulate the activity of actin in the cytoplasm. In G-actin, latrunculin is tightly bound to a pocket formed by α5 and α6 of the D4 subdomain and multiple hydrophobic residues in the D2 subdomain (34, 35). In N-actin, the twisting of the pointed end disrupts the latrunculin-binding pocket, with α5 moving into the binding pocket and α6 withdrawing from it (Fig. 3*B*). This structure suggests that the N-actin complex disfavors the binding of the drug. To confirm this inference, we compared the binding of latrunculin to the N-actin complex and G-actin by using biolayer interferometry (BLI). The data showed that latrunculin binds to G-actin, with a

disassociation constant (K_d) ~1 μM, consistent with an earlier measurement (36) (Fig. S6). By contrast, the N-actin complex did not interact with latrunculin, and no binding was observed even in the presence of 20 μM of the drug. These results are consistent with our model that the reshaped pointed end of N-actin disfavors the binding of latrunculin. Our findings differ from the previous suggestion that latrunculin targets N-actin within the BAF complex (5). This difference might be due to how the complexes were purified. Alternatively, the drug might bind to subunits of the BAF complex other than N-actin.

The barbed end of actin is the key element mediating its interactions with many ABPs, including profilin and cofilin, which are considered to regulate the dynamics of actin in the nucleus (5, 23). The superposition of actin in the complex with profilin or cofilin leads to severe clashes between the HSA domain and the bound ABPs (Fig. 3*C* and Fig. S7) (37, 38). The crystal structure of N-actin suggests that, within the chromatin-remodeling complex, it cannot interact with barbed end-binding proteins. To test this notion directly, we performed pull-down assays in vitro. Whereas GST-tagged profilin bound strongly to G-actin, it failed to interact with the N-actin complex (Fig. S8). These results are consistent with a recent report showing that N-actin within the Ino80 complex does not bind profilin (25), but differ from an earlier observation that the BAF complex binds to profilin (5). The reason for this difference is unknown. Our findings suggest the association between the BAF complex and profilin might be achieved through subunits other than N-actin or Arp4.

Thus, once bound to Arp4 and HSA^{Swr1}, N-actin has several structural features, which distinguish it from cytoplasmic actin and inhibit its interaction with many ABPs. The N-actin molecule within other chromatin remodeling complexes should have similar features given the strong homology of the complex components.

N-Actin Within Remodeling Complexes Is in the Nucleotide-Free apo State. Critically, the nucleotide-binding pocket of N-actin is blocked. The movement of the loop (Ser155–Thr160) in subdomain D3 causes the side chain of Asp157 to insert into the nucleotide-binding pocket, thus preventing the binding of any nucleotide at this site (Fig. 3*D*). Therefore, N-actin complexed with Arp4 and the HSA domain is in a nucleotide-free apo state. However, Arp4 tightly binds ATP within the same complex (Fig. S9*A*). These results suggest that the lack of a nucleotide within N-actin is not due to nucleotide loss during sample preparation or a crystallographic artifact (Fig. S9*B*). Instead, it is an intrinsic property of N-actin once it is assembled into the chromatin-remodeling complex.

The loss of the nucleotide from N-actin is surprising because it has long been known that actin in the nucleotide-free, apo state denatures rapidly (39, 40). To confirm the structural model, we performed ATP-exchange assays and examined the binding of ATP to N-actin. Consistent with previous results, the exchange of fluorescent ε-ATP with the ATP bound within G-actin increased the fluorescence intensity (41) (Fig. 3*E*). By contrast, no increase in fluorescence intensity was detected in the presence of the N-actin complex. These results support the idea that N-actin within the ternary complex does not bind ATP. These data also suggest that ATP bound by Arp4 is not readily released, consistent with an earlier study that showed ATP is intimately associated with Arp4 (14). To test the requirement of ATP binding for the actin–Arp4 interaction in cells, we introduced a G13R mutant human β-actin into HEK293 cells. The G13R mutation disrupts the ATP-binding pocket and reduces the stability of the protein (31). As expected, the mutant did not polymerize in cells (Fig. S4). However, it maintained its ability to interact with Arp4 (Fig. 2 *E* and *F*), consistent with the idea that nucleotide binding is not required by N-actin to associate with Arp4.

The absence of nucleotide in N-actin is intriguing. No nucleotide was found in the ARP subunits in the crystal structure of the Arp7–Arp9–HSA^{Snf2}–Rtt102 complex (26). A recent biochemical analysis showed that one ATP is bound to a single site within the Arp7–Arp9–HSA^{Sth1}–Rtt102 complex, presumably by the Arp7 subunit. This result is consistent with our observation that ATP is tightly bound by Arp4, whereas the nucleotide-binding pocket of N-actin remains empty. The similar nucleotide-binding mode of the actin/Arp4 and Arp7/9 pairs (Arp4 and Arp7 are in the ATP-bound state, whereas N-actin and Arp9 are in the apo state) further strengthens their conservation. It has been suggested that N-actin is regulated by the bound nucleotide (22, 25). However, the structure suggests that N-actin within the chromatin-remodeling complex does not bind any nucleotide, freeing it from regulation by ATP hydrolysis. Because Arp4 does not show detectable ATPase activity (42), these results suggest that ATP hydrolysis by the actin/ARP module may play a less important role in controlling the activity of the chromatin-remodeling complexes than what was previously proposed (22, 25). Instead, we speculate that ATP depletion and the nuclear accumulation of actin under stress conditions might act as signals to up-regulate the activity of the chromatin-remodeling complexes (43).

Implications for the Functions of N-Actin. Our structure shows that N-actin binds to the C-terminal end of the HSA domain, which is connected to the ATPase core domain of the remodeler. This structure suggests that N-actin may interact with the proximal catalytic core. This notion is consistent with a low-resolution map of the Swr1 holocomplex, in which the actin/Arp4 pair is close to the catalytic module (44). Alternatively, its close proximity to the catalytic core may allow N-actin to bind to the chromatin substrate, as suggested (25). Because the resolution of the map is limited, the precise interactions are unknown. More work is required to determine the interactions and specific functions of N-actin.

In summary, N-actin within the chromatin-remodeling complex has several important structural features, including a more twisted pointed end and a blocked barbed end. Additionally, it is not regulated by ATP hydrolysis. These unique features of N-actin distinguish it from its cytoplasmic counterpart and lay the groundwork for future studies of its functions inside the nucleus.

Materials and Methods

Protein Expression, Purification, Crystallization, and Structure Determination. For a detailed description of protein purification and related structure determination, see *SI Materials and Methods*. Briefly, *S. cerevisiae* Swr1 protein (amino acids 340–410) was expressed in *E. coli*. The full-length sequence of yeast actin and Arp4 were expressed in insect cells. Crystals were grown at 18 °C with the hanging-drop vapor diffusion method. Diffraction data were collected at beamline BL17U1 at the Shanghai Synchrotron Radiation Facility. The structure was solved by molecular replacement, and the final model was refined to 2.8 Å, with R_{work}/R_{feee} = 0.25/0.29.

Cellular Localization and Coimmunoprecipitation. HeLa cells and HEK293 cells were transferred with various actin constructs as described in *SI Materials and Methods*. The EGFP signal (HEK293 cells) was visualized directly 48 h after transfection. The HeLa cells were fixed with 4% (wt/vol) paraformaldehyde 48 h after transfection. A primary mouse anti-GFP monoclonal antibody and a goat anti-mouse IgG polyclonal secondary antibody conjugated to Alexa Fluor 488 were used for immunofluorescence detection.

HEK293 cells transfected with various actin constructs were harvested 48 h after transfection and lysed in hypotonic buffer. The nuclear extract was resuspended and then incubated with anti-Flag beads (M2; Sigma). After washing, samples were eluted with SDS loading buffer and analyzed with Western blotting by using antibodies specific for the Flag tag (Cell Signaling) and Arp4 (ACLT6A; Abcam). At least five independent experiments were performed, and representative blots are shown.

Nucleotide Exchange Assays, GST Pull-Down Assays, and BLI. For a detailed description of the assays, see *SI Materials and Methods*. The fluorescent

signal from 1,N^6-ethenoadenosine 5′-triphosphate (ε-ATP; Jena Bioscience) bound to actin was used to measure the rate of exchange of the actin nucleotide (45). Briefly, ε-ATP (50 μM) was added to the solution of 3 μM G-actin or the N-actin complex. The reaction was monitored with a Quanta-Master Luminescence QM 3 PH Fluorometer.

GST-tagged profilin (5 μM) was mixed with 10 μM G-actin or the N-actin complex and then incubated with GST resin. The resin was washed three times and then eluted. The samples were analyzed with SDS/PAGE and stained with Coomassie blue.

An Octet RED BLI instrument (FortéBio) was used to examine the binding of latrunculin to G-actin or the N-actin complex. We exposed the biosensors to different concentrations of latrunculin in the association step and then washed the biosensors with buffer in the dissociation step. The BLI data were fitted with the Octet Data analysis software package and graphed with the Origin 8.0 software.

ACKNOWLEDGMENTS. We thank Shilong Fan at the center of structure biology (Tsinghua University) and the staff at beamline BL17U of Shanghai Synchrotron Radiation Facility for help with diffraction data collection and the Tsinghua University Branch of China National Center for Protein Sciences Beijing for providing facility support. This work was supported by Chinese Key Research Plan-Protein Sciences Grant 2014CB910100, National Natural Science Foundation of China Grant 31270762, and the "Junior One Thousand Talents" program (to Z.C.).

1. Pollard TD, Cooper JA (2009) Actin, a central player in cell shape and movement. *Science* 326(5957):1208–1212.
2. Volkmann N, et al. (2001) Structure of Arp2/3 complex in its activated state and in actin filament branch junctions. *Science* 293(5539):2456–2459.
3. Olave IA, Reck-Peterson SL, Crabtree GR (2002) Nuclear actin and actin-related proteins in chromatin remodeling. *Annu Rev Biochem* 71:755–781.
4. Pederson T, Aebi U (2002) Actin in the nucleus: What form and what for? *J Struct Biol* 140(1-3):3–9.
5. Zhao K, et al. (1998) Rapid and phosphoinositol-dependent binding of the SWI/SNF-like BAF complex to chromatin after T lymphocyte receptor signaling. *Cell* 95(5):625–636.
6. Galarneau L, et al. (2000) Multiple links between the NuA4 histone acetyltransferase complex and epigenetic control of transcription. *Mol Cell* 5(6):927–937.
7. Shen X, Mizuguchi G, Hamiche A, Wu C (2000) A chromatin remodelling complex involved in transcription and DNA processing. *Nature* 406(6795):541–544.
8. Ikura T, et al. (2000) Involvement of the TIP60 histone acetylase complex in DNA repair and apoptosis. *Cell* 102(4):463–473.
9. Clapier CR, Cairns BR (2009) The biology of chromatin remodeling complexes. *Annu Rev Biochem* 78:273–304.
10. Szerlong H, et al. (2008) The HSA domain binds nuclear actin-related proteins to regulate chromatin-remodeling ATPases. *Nat Struct Mol Biol* 15(5):469–476.
11. Kosho T, Miyake N, Carey JC (2014) Coffin-Siris syndrome and related disorders involving components of the BAF (mSWI/SNF) complex: Historical review and recent advances using next generation sequencing. *Am J Med Genet C Semin Med Genet* 166C(3):241–251.
12. Kadoch C, Crabtree GR (2015) Mammalian SWI/SNF chromatin remodeling complexes and cancer: Mechanistic insights gained from human genomics. *Sci Adv* 1(5):e1500447.
13. Wilson BG, Roberts CW (2011) SWI/SNF nucleosome remodellers and cancer. *Nat Rev Cancer* 11(7):481–492.
14. Fenn S, et al. (2011) Structural biochemistry of nuclear actin-related proteins 4 and 8 reveals their interaction with actin. *EMBO J* 30(11):2153–2166.
15. Bird AW, et al. (2002) Acetylation of histone H4 by Esa1 is required for DNA double-strand break repair. *Nature* 419(6905):411–415.
16. Downs JA, et al. (2004) Binding of chromatin-modifying activities to phosphorylated histone H2A at DNA damage sites. *Mol Cell* 16(6):979–990.
17. Yoo AS, Staahl BT, Chen L, Crabtree GR (2009) MicroRNA-mediated switching of chromatin-remodelling complexes in neural development. *Nature* 460(7255):642–646.
18. Lessard J, et al. (2007) An essential switch in subunit composition of a chromatin remodeling complex during neural development. *Neuron* 55(2):201–215.
19. Wu JI, et al. (2007) Regulation of dendritic development by neuron-specific chromatin remodeling complexes. *Neuron* 56(1):94–108.
20. Krasteva V, et al. (2012) The BAF53a subunit of SWI/SNF-like BAF complexes is essential for hemopoietic stem cell function. *Blood* 120(24):4720–4732.
21. Kapoor P, Shen X (2014) Mechanisms of nuclear actin in chromatin-remodeling complexes. *Trends Cell Biol* 24(4):238–246.
22. Percipalle P, Visa N (2006) Molecular functions of nuclear actin in transcription. *J Cell Biol* 172(7):967–971.
23. Blessing CA, Ugrinova GT, Goodson HV (2004) Actin and ARPs: Action in the nucleus. *Trends Cell Biol* 14(8):435–442.
24. Rando OJ, Zhao K, Janmey P, Crabtree GR (2002) Phosphatidylinositol-dependent actin filament binding by the SWI/SNF-like BAF chromatin remodeling complex. *Proc Natl Acad Sci USA* 99(5):2824–2829.
25. Kapoor P, Chen M, Winkler DD, Luger K, Shen X (2013) Evidence for monomeric actin function in INO80 chromatin remodeling. *Nat Struct Mol Biol* 20(4):426–432.
26. Schubert HL, et al. (2013) Structure of an actin-related subcomplex of the SWI/SNF chromatin remodeler. *Proc Natl Acad Sci USA* 110(9):3345–3350.
27. Oda T, Iwasa M, Aihara T, Maéda Y, Narita A (2009) The nature of the globular- to fibrous-actin transition. *Nature* 457(7228):441–445.
28. Holmes KC, Popp D, Gebhard W, Kabsch W (1990) Atomic model of the actin filament. *Nature* 347(6288):44–49.
29. Fujii T, Iwane AH, Yanagida T, Namba K (2010) Direct visualization of secondary structures of F-actin by electron cryomicroscopy. *Nature* 467(7316):724–728.
30. Szerlong H, Saha A, Cairns BR (2003) The nuclear actin-related proteins Arp7 and Arp9: A dimeric module that cooperates with architectural proteins for chromatin remodeling. *EMBO J* 22(12):3175–3187.
31. Posern G, Sotiropoulos A, Treisman R (2002) Mutant actins demonstrate a role for unpolymerized actin in control of transcription by serum response factor. *Mol Biol Cell* 13(12):4167–4178.
32. Rao JN, Madasu Y, Dominguez R (2014) Mechanism of actin filament pointed-end capping by tropomodulin. *Science* 345(6195):463–467.
33. Irobi E, et al. (2004) Structural basis of actin sequestration by thymosin-beta4: Implications for WH2 proteins. *EMBO J* 23(18):3599–3608.
34. Morton WM, Ayscough KR, McLaughlin PJ (2000) Latrunculin alters the actin-monomer subunit interface to prevent polymerization. *Nat Cell Biol* 2(6):376–378.
35. Belmont LD, Patterson GM, Drubin DG (1999) New actin mutants allow further characterization of the nucleotide binding cleft and drug binding sites. *J Cell Sci* 112(Pt 9):1325–1336.
36. Yarmola EG, Somasundaram T, Boring TA, Spector I, Bubb MR (2000) Actin-latrunculin A structure and function. Differential modulation of actin-binding protein function by latrunculin A. *J Biol Chem* 275(36):28120–28127.
37. Schutt CE, Myslik JC, Rozycki MD, Goonesekere NC, Lindberg U (1993) The structure of crystalline profilin-beta-actin. *Nature* 365(6449):810–816.
38. Paavilainen VO, Oksanen E, Goldman A, Lappalainen P (2008) Structure of the actin-depolymerizing factor homology domain in complex with actin. *J Cell Biol* 182(1):51–59.
39. Asakura S (1961) The interaction between G-actin and ATP. *Arch Biochem Biophys* 92:140–149.
40. Kasai M, Nakano E, Oosawa F (1965) Polymerization of actin free from nucleotides and divalent cations. *Biochim Biophys Acta* 94:494–503.
41. Pollard TD, Goldberg I, Schwarz WH (1992) Nucleotide exchange, structure, and mechanical properties of filaments assembled from ATP-actin and ADP-actin. *J Biol Chem* 267(28):20339–20345.
42. Gerhold CB, et al. (2012) Structure of Actin-related protein 8 and its contribution to nucleosome binding. *Nucleic Acids Res* 40(21):11036–11046.
43. Pendleton A, Pope B, Weeds A, Koffer A (2003) Latrunculin B or ATP depletion induces cofilin-dependent translocation of actin into nuclei of mast cells. *J Biol Chem* 278(16):14394–14400.
44. Nguyen VQ, et al. (2013) Molecular architecture of the ATP-dependent chromatin-remodeling complex SWR1. *Cell* 154(6):1220–1231.
45. Goldschmidt-Clermont PJ, et al. (1992) The control of actin nucleotide exchange by thymosin beta 4 and profilin. A potential regulatory mechanism for actin polymerization in cells. *Mol Biol Cell* 3(9):1015–1024.
46. Chen Z, et al. (2010) Structure and control of the actin regulatory WAVE complex. *Nature* 468(7323):533–538.
47. Kabsch W (2010) Xds. *Acta Crystallogr D Biol Crystallogr* 66(Pt 2):125–132.